ACS APPLIED MATERIALS & INTERFACES

Research Article

www.acsami.org

New Basic Insights into the Low Hot Electron Injection Efficiency of Gold-Nanoparticle-Photosensitized Titanium Dioxide

Xiangchao Ma,[†] Ying Dai,*[,†] Lin Yu,[†] and Baibiao Huang[‡]

[†]School of Physics, State Key Lab of Crystal Materials and [‡]State Key Lab of Crystal Materials, Shandong University, Jinan 250100, China

Supporting Information

ABSTRACT: The low hot electrons injection efficiency (HEIE) from plasmonic metal to semiconductor significantly affects the performance of metal−semiconductor composite. However, there are few reports about the origin of this low HEIE. In the present work, the factors affecting the transfer process and generation efficiency of hot electron in Au@TiO_2 composite are investigated using first-principles calculations and Maxwell's electrodynamics theory. The occupation of surface oxygen vacancies of TiO_2 by gold atoms is found to increase the hot electrons transfer barrier and expand the space charge region, which decrease the HEIE. In addition, the existing Au@TiO_2 structure going against the generation of large amount of hot electrons may also lead to low HEIE. Our results reveal that the replacement of divalent host oxygen atoms with monovalent atoms can decrease the HEIE and comparison with experimental results allows us to validate our predictions. Furthermore, proper surface treatment of semiconductor before depositing metal particles and structure optimization of the composite are suggested to improve the HEIE.

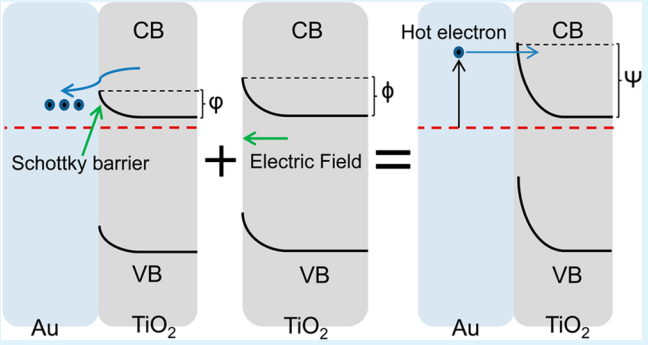

KEYWORDS: *photocatalysis, hot electron, injection efficiency, DFT calculations, titania*

1. INTRODUCTION

The metal−semiconductor composites have been extensively used for a wide variety of applications,[1−3] where the interfacial charge-transfer strongly affects their performance. Recently, plasmonic metal−semiconductor nanosystem, known as plasmonic photocatalyst, is introduced into photocatalysis.[1,4] In such system, the metal nanoparticles (NPs) strongly absorb visible light by surface plasmon resonance (SPR), which significantly enhances the light absorption efficiency of conventional semiconductor photocatalyst.[5] In effect, this design method can potentially establish a new paradigm in harvesting photons for practical use due to the easiness of manipulating SPR absorption of metal NPs. As for how the SPR helps to generate electrons and holes, it has been widely recognized that the hot electrons originating from the decay of SPR are injected into the conduction band (CB) of semiconductor, known as hot electron injection process,[6] leaving holes in the NPs. However, the hot electron injection efficiency (HEIE) is generally very low,[7,8] which significantly affects the overall photocatalytic performance and is commonly attributed to the Schottky barrier formed due to the electron transfer between semiconductor and metal. Despite this conventional opinion, taking the commonly used TiO_2 for example, the n-type conductivity of TiO_2 with the general carrier density of $10^{17}/cm^3$ is often induced unconsciously due to the inevitable formation of oxygen vacancies (Ovs),[9] the Schottky barrier φ resulting from electron transfer from n-type TiO_2 to gold (Au) NPs is estimated to be only about 0.6 eV according to the Schottky model.[10] Since it was suggested that the energy of hot electrons can be as high as 2 eV above the Fermi level,[11] the small Schottky barrier cannot fully account for the low HEIE (Figure 1a). In addition, considering the fact that if more hot electrons are expected to inject into the semiconductor, the amount of generated hot electrons moving toward the semiconductor in Au NPs should also play an important role in determining the HEIE in addition to the injection barrier.

Therefore, in fact, the physical origin of the low HEIE has been somewhat mysterious although the Schottky barrier does play partial role, and a comprehensive study of the low HEIE is urgently needed for improving performance of the system. Here, we present such a study. Because it is quite probable that Au atoms can occupy the surface Ovs of TiO_2 in the preparation of Au@TiO_2 by photoreducing a gold salt,[3,12] and recent experimental results showed that the photocatalytic performance of prepared Au@TiO_2 samples by direct deposition of presynthesized Au NPs is superior to that prepared by photoreducing method,[12] we examine if such occupation can affect the hot electron injection efficiency, which is generally overlooked, by performing sophisticated

Received: April 14, 2014
Accepted: July 28, 2014
Published: July 28, 2014

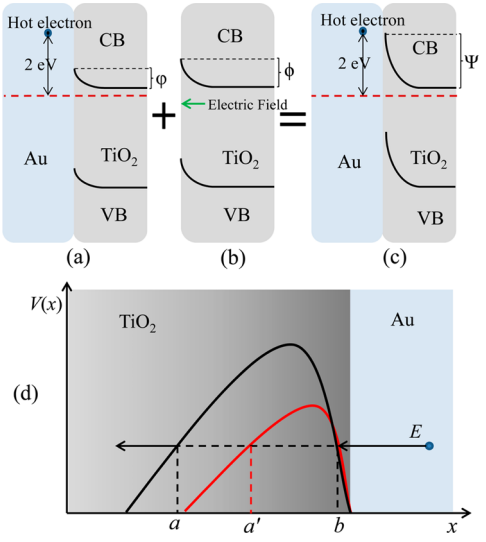

Figure 1. (a) Schottky barrier (φ) induced by charge transfer from n-type TiO_2 to Au. (b) Schematic of the upward band bending (ϕ) induced by the negatively charged surface atomic layers. (c) The final hot electron transfer barrier $\Psi = \phi + \varphi$. (d) Schematic of the spatial distribution of hot electrons transfer barrier ($V(x)$) with respect to the Au/TiO_2 interface normal before (the red curve) and after (the black curve) Au atoms occupy the surface Ovs; the hot electron transfer from the right to the left, as indicated with the arrowed line.

hybrid density functional calculations and thus affect the photocatalytic performance. In addition, because the hot electron generation efficiency is linked to light absorption efficiency of Au NPs, which also determine the near field enhancement,[13,14] the absorption efficiency along with the near field enhancement with respect to the direction of incident light are investigated by numerically solving Maxwell equations for model structure of Au@TiO_2. Our results provide compelling evidence that the occupation of surface divalent oxygen vacancy sites of semiconductor by monovalent Au atoms can increase the hot electrons transfer barrier and expand the space charge region, thus decreasing the HEIE. In addition, some guidelines to improve the HEIE are proposed.

2. COMPUTATIONAL DETAILS

The hybrid density functional calculations of TiO_2 with defects (Ov and Au@Ov) are based on the generalized Kohn–Sham theory and the projector-augmented wave potentials as implemented in the Vienna Ab Initio Simulation Package (VASP).[15,16] The lattice parameters of anatase TiO_2 [a = 3.776 Å, c/a = 2.512 Å] from experimental results[17] are used for our calculations. We employ the well-known HSE06 hybrid functional, which can provide good physical descriptions of defects in wide-bandgap semiconductors,[18,19] a $2\sqrt{2} \times 2\sqrt{2} \times 1$ supercell with 96 atoms to simulate bulk TiO_2 and a 2×2 (2×1) supercell slab with 72 (126) atoms to describe the {101} (1×4 reconstructed {001}) surface, which can well minimize the possible interaction between neighboring defects,[9] and a 20 Å thickness of vacuum layer to avoid the interaction between repeated slabs, the cutoff energy of 400 eV for the plane wave expansion and the $2 \times 2 \times 2$ ($2 \times 2 \times 1$) Γ-centered k-points[20] for sampling the Brillouin zone of TiO_2 bulk (surface), which are found to be large enough for energy convergence. The possible dipole moment induced upon occupation of gold atom in surface oxygen vacancy is also taken into account using a dipole correction in our calculations. The positions of all atoms are fully relaxed until the residual force is smaller than 0.02 eV/Å. The densities of states (DOS) are calculated at the equilibrium volume using the tetrahedron method with Blöchl corrections for accuracy.[21]

The electronic properties of Ov in bulk TiO_2 are investigated by estimating the formation energies and thermodynamic donor levels. The formation energy of a Ov in charge state q is defined as[22]

$$E_f(V_O^q) = E(V_O^q) - E(\text{host}) + \frac{1}{2}E(O_2) + qE_F$$

where $E(\alpha)$ is the total energy of fully relaxed system α. The reference for oxygen energy is given by an O_2 molecule considering the oxygen rich condition. The last term in the formation energy accounts for the fact that O_V^+/O_V^{2+} donates one/two electrons, E_F denotes the energy of the reservoir with which these electrons are exchanged and is equal to the Fermi level of the system. Any Makov–Payne-like correction is negligible given the high dielectric constant of TiO_2.[23] The donor levels of $\varepsilon(+1/0)$ and $\varepsilon(+2/+0)$ are defined as the Fermi level position where the formation energies of charge states +1/+2 and 0 are equal.[22] We note that although the donor levels are estimated in the oxygen rich condition, they do not change with condition,[9] and only the formation energies of the systems change with respect to the condition.

The SPR properties including the SPR optical absorption and near field enhancement of Au@TiO_2 are calculated by numerically solving the Maxwell's equations using the discrete dipole approximation (DDA) as implemented in the DDSCAT code.[24,25] The DDA simulates an object of certain size and shape with certain refractive index by using an array of polarizable points. A gold sphere with the diameter of 20 nm comparable with experimentally prepared samples is used in our calculations. The TiO_2 substrate is represented by a slab of TiO_2 with certain thickness after systematically checking how the slab thickness affects the results of our DDA calculations until use of a thicker slab does not significantly affect the results. In our DDA calculations, the wavelength-dependent refractive indices of Au are taken from ref 26 with the refractive index of 2.4 for TiO_2,[27] and water is used as the external dielectric medium since the Au@TiO_2 catalyst generally functions in aqueous solutions. For the full convergence of the DDA calculations, an interdipole distance shorter than 1 nm is used. The absorption efficiency is given by the ratio of the absorption cross-section to the geometrical cross-section $\pi(a_{eff})^2$, where the "effective radius" a_{eff} is the radius of a sphere equal in volume to the specific model structure under examination.

3. RESULTS AND DISCUSSION

3.1. Donor Properties of Ovs in TiO_2. First of all, it is important to identify the donor properties of Ovs in TiO_2. Although it has been widely accepted that Ovs are the cause of n-type conductivity of TiO_2 experimentally,[9,28] there have been few works regarding the thermodynamic donor levels of Ovs[9,29,30] Mattioli et al. recently reported that the thermodynamic donor levels of Ovs in anatase TiO_2 are very shallow; however, their accurate values depend on the Hubbard U used in the GGA+U calculations.[23] In this work, we reestimate the thermodynamic donor levels of Ovs using state of the art hybrid density functional calculations. As shown in Figure 2, the donor levels of both $\varepsilon(+1/0)$ and $\varepsilon(+2/0)$ are found to be resonant with host CB, which strongly confirm the existing experimental and theoretical predictions. Moreover, the formation energy of oxygen vacancy (Ov) in +2 charge state is well lower than that of the ones in +1 and 0 charge states all across the band gap, hence Ovs in bulk region should be generally in +2 charge states in thermodynamic equilibrium. These results apparently suggest that Ovs in bulk region can effectively donate the initial two electrons into host CB functioning as double donors. For Ovs on the surface, the donor levels should be located in energy much higher than that of bulk ones, since the shallow donor levels of Ovs are actually a consequence of the structural relaxation of adjacent Ti atoms[9]

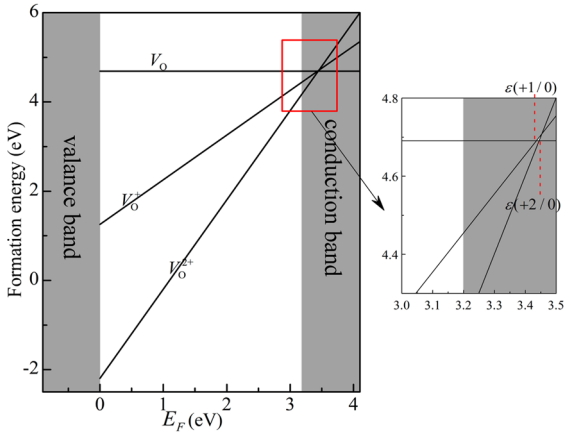

Figure 2. Formation energies of oxygen vacancy (Ov) in different charge states in anatase TiO_2 as a function of Fermi level in O-rich condition. The donor levels of $\varepsilon(+1/0)$ and $\varepsilon(+2/0)$ are indicated with red dashed lines.

and the surface Ti atoms have larger relaxation than the bulk ones.

3.2. Effects of Au Atoms Occupying the {101} Surface Ovs of TiO_2. As outlined in the introduction, experimental preparation of Au@TiO_2 plasmonic photocatalyst by photoreducing method makes it quite probable that most of the surface Ovs are occupied by Au atoms. However, although a great deal of effort is devoted to the study of TiO_2 surface Ovs,[29−32] little attention has been paid to the occupation of Ov by Au atom, and only Selloni et al.[33] slightly described the bonding structures of one case of Au atom occupying Ov on {101} surface. In this part, we systematically examine the geometric and electronic structures of Au atoms occupying all of the possible surface Ovs of TiO_2 nanocrystal.

On {101} surface, there are three different surface Ov sites. The bond lengths between Au and adjacent Ti atoms for the three cases of Au atoms occupying surface Ovs are approximately equal to the sum of the covalent radii of Au (1.34 Å) and Ti (1.32 Å) (Table 1), suggesting that they are

Table 1. Local Bond Lengths between Au and Adjacent Ti Atoms[a]

structure	Au−Ti1 (Å)	Au−Ti2 (Å)
Au@Ov1	2.54	2.86
Au@Ov2	2.93	2.64
Au@Ov3	2.47	2.69

[a]Note that the atom numbers (Ti1 and Ti2) correspond to that in Figure 3.

chemically bonding with each other. In addition, the Au atoms significantly deviate from the original oxygen sites (Figure 3), which is probably linked to the larger atomic radius of Au compared to that of O (1.79 vs 0.91 Å). To gain insight into the bonding nature, their detailed electronic structures are investigated. In all of the three cases, the most notable effect of Au atoms occupying the surface Ovs is that some gap states above the valence band maximum (VBM) are induced and the gap states are mainly composed of Au *s* states only with slight states of adjacent Ti atoms (Figure 3). This means that one of the two electrons donated by Ov is transferred to Au *s* orbital forming somewhat ionic bonding between Au and adjacent Ti atoms, which is also verified by the charge density distributions

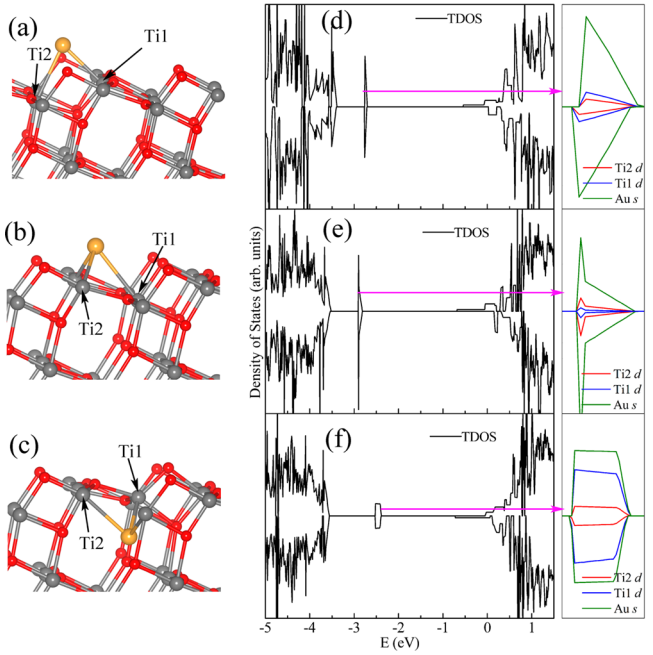

Figure 3. Local geometric structures and electronic density of states (DOS) of Au atoms occupying the three Ovs on {101} surface. Parts a, b, and c are the optimized geometric structures of Au atoms occupying the three Ovs on {101} surface, hereafter referred to as Au@Ov1, Au@Ov2, and Au@Ov3, respectively. Parts d, e, and f are the corresponding total DOS (on the left) and projected DOS of the gap states (on the right). The Fermi level is set to 0 eV.

of the gap states (Figure 4). This result is attributed to the much larger electronegativity of Au than that of Ti (2.54 vs 1.54 in Pauling scale).[34]

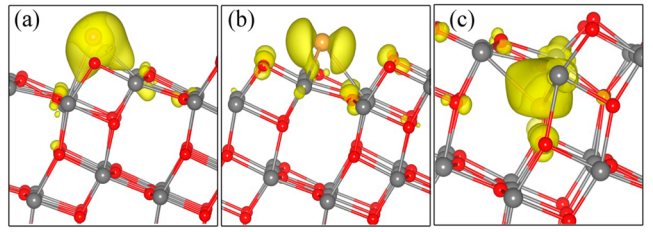

Figure 4. Electronic charge density distribution of the bonding states of Au with adjacent Ti atoms as Au atoms occupy the surface Ovs of {101}. (a) For Au@Ov1. (b) For Au@Ov2. (c) For Au@Ov3. The isosurfaces are at 0.008 electrons $Å^{-3}$ in all of the three cases.

The implications of the strong bonding between Au and adjacent Ti atoms are as follows: (1) there should be strong electrostatic repulsion between the negatively charged Au and neighboring O atoms, which can also contribute to the deviation of Au atom from the original oxygen site; (2) The original shallow double donor (Ov) is eventually transformed into single donor; Thus, in thermodynamic equilibrium, some of the electrons donated by bulk region Ovs have to populate the surface region to keep the Fermi level uniform across the nanocrystal, making the surface region negatively charged. The impact of such negatively charged surface region on HEIE will be discussed later.

We have reported the bonding states of Au with adjacent Ti atoms. Now, we examine their antibonding states. As shown in Figure 5, the antibonding states of the three cases are mainly

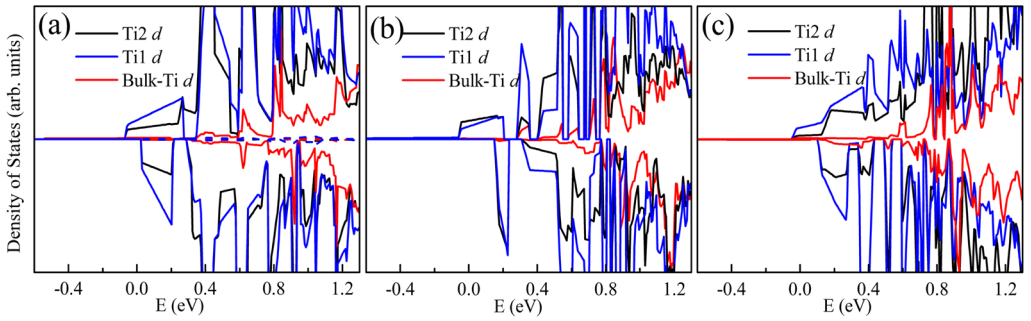

Figure 5. Electronic density of states (DOS) for the *d* states of Ti bonding with Au on {101} surface and that in the bulk region. (a) For Au@Ov1. (b) For Au@Ov2. (c) For Au@Ov3. Note that the atom numbers (Ti1 and Ti2) correspond to that in Figure 3. The Fermi level is set to 0 eV.

composed of Ti *d* states and located quite lower in energy than the antibonding states (which form host CB) of Ti−O in the inner atomic layers. The bonding process of Au with adjacent Ti atoms based on the molecular orbital theory can legitimatize these behaviors (Figure 6): As the O 2*p* orbital lies quite lower

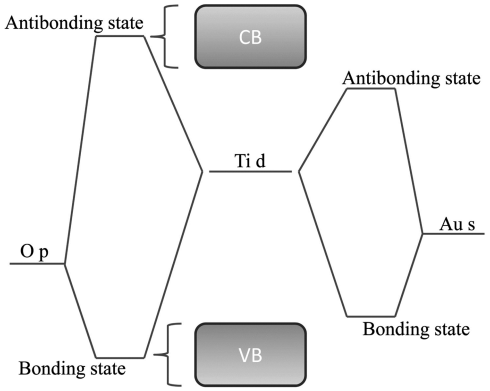

Figure 6. Details of orbital interaction of Ti with O and Au on the basis of molecular orbital theory.

in energy than the Au 6*s* orbital, the bonding between Au and Ti must be weaker than that between O and Ti. As a consequence, their bonding states lie higher in energy than that between O and Ti, which can explain the location of the bonding states between Au and Ti above the host VBM. On the other hand, their antibonding states should lie lower in energy than those of Ti−O. Therefore, some electron carriers in the host CB will be trapped in the unoccupied antibonding states between Au and adjacent Ti atoms in thermal equilibrium, which can further increase the negative charge of surface atomic region. These negatively charged surface atomic layers can adversely impact the hot electrons transfer from Au NPs to TiO_2 substrate.

The negatively charged surface atomic layers can decrease HEIE through the well increased hot electron transfer barrier and extended space charge region. Similar to the formation mechanism of Schottky barrier,[10] where a large positively charged region known as space charge region forms when some electrons in n-type TiO_2 move to the Au NPs, the negatively charged surface region can also induce quite a large positively charged inner region. Thus, an electric field pointing to the surface is induced, which can result in upward band bending (Figure 1b). The superposition of this band bending with the Schottky barrier can result in a larger hot electron transfer barrier and space charge region (Figure 1c). Here, it is noted that assertion of the increase of hot electron transfer barrier is mostly based on the effects of Au atoms occupying the surface Ovs on the electron distributions across the TiO_2 substrate in thermodynamic equilibrium. Although the real charge distributions on Au atoms and TiO_2 host as large amount of electrons populate the TiO_2 conduction band cannot be simulated by DFT calculations at the moment, it is believed that the electronic structures of Au atoms occupying surface Ovs can provide a solid basis for reasonable inferences of the charge distributions. Theoretically, the extent to which the negatively charged surface atomic layers can increase the transfer barrier and extend the space charge region may be obtained by solving the Poisson equation;[10] however, due to the lack of appropriate model describing the positive charge distribution in the inner region, the extent is not estimated here. The effects of the increased hot electron transfer barrier and extended space charge region on HEIE can be estimated as follows: When the energy of hot electron is smaller than the peak value of the transfer barrier, HEIE can be approximately given by the following equation on the basis of WKB approximation[35]

$$\eta = \exp\left[-\frac{2}{\hbar}\left|\int_a^b \sqrt{2m(E - V(x))}\,\mathrm{d}x\right|\right]$$

where E and $V(x)$ are the energy of hot electron and the spatial distribution of hot electron transfer barrier (Figure 1d), respectively; m is the effective mass of incident electron; $\hbar$ is the reduced Planck constant; the integrating range between a and b corresponds to the range between the entry and exit points when hot electron with energy E moves across the transfer barriers, as indicated in Figure 1d. It is noted that Figure 1d is schematic illustrations of the spatial distribution of conduction band level of TiO_2 near the interface from Figure 1a and c. On the other hand, when the hot electron energy approaches or becomes larger than the peak value of the transfer barrier, the HEIE can be estimated according to a modified Fowler formula, as proposed in the work of Giugni et al.[36] Then, it can be readily concluded that the HEIE can be reduced due to superposition of the two kind of barriers.

3.3. Effects of Au Atoms Occupying the Reconstructed {001} Surface Ovs of TiO_2. To make our study more comprehensive and reflect the experimental results more accurately, the cases of Au atoms occupying the surface Ovs of the widely accepted (1 × 4) reconstructed {001} surface[37] are also examined. The bond lengths and bonding nature of Au occupying the six accessible surface Ovs are very similar to that on the {101} surface because of similar physical origin (Supporting Information (SI) Figures S1 and S2; Table S1), except that the antibonding states between Au and adjacent Ti are quite different from that on the {101} surface. Their

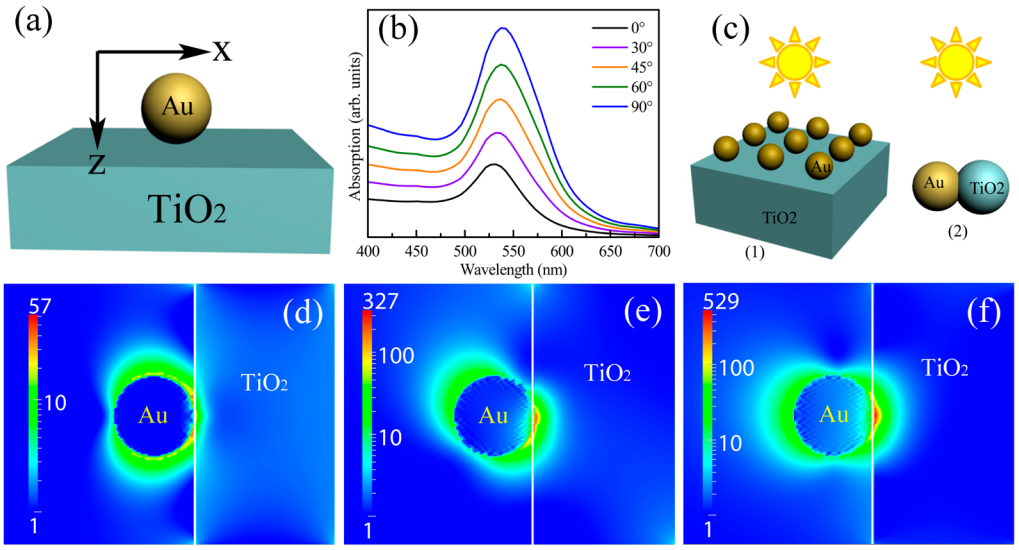

Figure 7. (a) Relative positions of Au nanoparticle and TiO_2 substrate and the coordinates we use in our description. (b) The calculated SPR absorption spectra of the Au@TiO_2 model for incident light in different directions. The incident light direction is indicated by the intersection angle between the incident light direction and z direction as indicated in part a. (c) Schematics of the realistic Au@TiO_2 system (1) and the proposed Au@TiO_2 system (2), which should be beneficial to the generation of more hot electrons. (d, e, f) Near field enhancement, namely, E^2/E_0^2, for incident light with the intersection angle of 0°, 45°, and 90°, respectively.

antibonding states are located just slightly lower or even higher in energy than the host Ti−O antibonding states (SI Figure S3). Thus, the further increased negative charge due to charge trapping by the unoccupied antibonding states as found on {101} surface is alleviated to some extent.

We have revealed that the occupation of Ovs on the generally exposed TiO_2 nanocrystal surfaces by Au atoms can significantly reduce the HEIE. Bian et al. recently reported quite different photocatalytic performance of the prepared Au@TiO_2 samples using two different methods,[12] where the photoreducing method can make Au atoms occupy more surface Ovs of TiO_2 than the other method does; therefore, the sample prepared by photoreducing method should show lower photocatalytic performance due to the reduced HEIE, which is in agreement with experimental results.[12] This result also suggests that removing the surface Ovs before metal NPs loading can improve the HEIE to some extent.

There are two main channels for the energy transfer from Au NPs to TiO_2: the hot electron injection and near field enhancement of the light absorption of semiconductor. Therefore, although the hot electron injection channel may be hampered by photoreducing method, the prepared samples can still show relatively good photocatalytic performance because of the SPR near field enhancement. Our present results suggest that further enhancement of the photocatalytic performance may be achieved by methods preventing the occupation of Au atoms in the surface Ovs and thus releasing the hot electron injection channel. For example, Miljevic et al. recently reported enhanced photocatalytic performance of Au@TiO_2 prepared using bifunctional bridging linker, which can well decrease the probability of Au atoms occupying the surface Ovs[38]

3.4. Hot Electron Generation Efficiency in Au Nanoparticles Deposited on TiO_2 Substrate. As outlined in the introduction, the generation efficiency of hot electrons, which also plays an important role in determining the HEIE, is associated with the SPR light absorption efficiency and near field enhancement. Our recent work has shown the SPR absorption efficiency and near field enhancement with respect to the various shapes and sizes of silver NPs on AgCl semiconductor,[39] and therefore, similar SPR properties of Au NPs in various shapes and sizes on TiO_2 substrate can be expected because of the same underling mechanism. Here, we mainly focus our attention on the SPR properties with respect to the direction of incident light, which may provide insights into the effect of the structures of metal−semiconductor composite on generation of hot electrons moving toward the semiconductor substrate.

To facilitate our interpretation, the relative structures of Au nanoparticle and TiO_2 substrate and the coordinates we use are shown in Figure 7a. Our calculated SPR wavelength at about 535 nm is in agreement with the experimental results (Figure 7b).[6,12,40] Most notably, the absorption efficiency increases steadily as the incident direction of light varies from z direction to x direction. Here, we note that the absorbed incident light along the z direction can make none of the generated hot electrons move toward the semiconductor substrate according to the conservation of momentum.[8,14] Therefore, the composite structure of Au/TiO_2, which is beneficial for the system to absorb light traveling in the directions other than the Au/TiO_2 interface normal (which is the z direction) should help to generate many more hot electrons with the "right" momentum. Since the semiconductor substrate is significantly larger than the metal NPs in the commonly prepared Au@TiO_2 composite (Figure 7c(1)),[38] it is mostly the incident light propagating approximately along the interface normal that are absorbed, then the optical electric field will be almost parallel to the interface because electromagnetic wave is transverse wave. Therefore, the relative weak light absorption efficiency and near field enhancement, as shown in Figure 7b and d, may be not beneficial to generation of a large number of hot electrons. We propose that an Au@TiO_2 system composed of Au and TiO_2 NPs in comparable dimensions (Figure 7c(2)), which is beneficial for the system to absorb light traveling in the directions other than the Au/TiO_2 interface normal, should help to generate more hot electrons. In addition, it is noted that

the intensity and distribution range of near field in the semiconductor also increase as the incident direction of light varies from z to x direction (Figure 7d–f), thus the near field enhanced energy transfer process can also be increased.[41] These results apparently suggest that a win–win situation for SPR energy transfer from metal to semiconductor can eventually be obtained by designing proper structure of the composite. The present results can also contribute to understand the experimental results that photocatalytic activities of Au@TiO_2 samples depend strongly on the relative sizes of Au and TiO_2 NPs.[42]

4. CONCLUSION

In summary, we found that in all cases of Au occupying the surface Ovs of {101} and {001} surfaces, the initially shallow double donors are eventually transformed into single donors and unoccupied antibonding states are also introduced into the energy gap of TiO_2, which make the surface atomic layers of TiO_2 nanocrystals negatively charged in thermodynamic equilibrium. Thus, upward band bending is induced, which increases the hot electron transfer barrier and expand the space charge region. As a result, the hot electron injection efficiency is quite low. Our findings provide new ways to understand the recent experimental results.[12] In addition, the general structure of Au@TiO_2, where Au NPs are deposited on a relatively large TiO_2 substrate, is found to be not beneficial for the generation of large amount of hot electrons moving toward the semiconductor substrate, which also results in low hot electron injection efficiency. We propose some guidelines for structure optimization of the composite, which should not only help to improve the HEIE but also be beneficial for light absorption and near field enhanced energy transfer process.

Most notably, to our knowledge, there are few reports about the low hot electron injection efficiency theoretically. Our results provide compelling evidence about the effect of occupation of surface Ovs by Au atoms on electron transfer between metal and semiconductor and it is believed that similar results should also exist in systems where monovalent noble metal atoms can substitute the semiconductor host multivalent atoms.

■ ASSOCIATED CONTENT

Supporting Information

Local geometrical structures and electronic structures of Au atoms occupying the surface oxygen vacancies of the (1 × 4) reconstructed {001} surface. This material is available free of charge via the Internet at http://pubs.acs.org.

■ AUTHOR INFORMATION

Corresponding Author

*Email: daiy60@sina.com.

Notes

The authors declare no competing financial interest.

■ ACKNOWLEDGMENTS

This work is supported by the National Basic Research Program of China (973 program, 2013CB632401), National Science Foundation of China (grants 11374190 and 21333006), the Natural Science Foundation of Shandong Province (grants ZR2011AM009 and ZR2013AM021), and 111 Project B13029. We also thank the National Supercomputer Centre in Jinan and High Performance Computing Centre of Shandong University for providing high performance computation.

■ REFERENCES

(1) Wang, P.; Huang, B.; Qin, X.; Zhang, X.; Dai, Y.; Wei, J.; Whangbo, M.-H. Ag@AgCl: A Highly Efficient and Stable Photocatalyst Active under Visible Light. *Angew. Chem., Int. Ed.* **2008**, *47*, 7931–7933.

(2) Wu, Y.; Xiang, J.; Yang, C.; Lu, W.; Lieber, C. M. Single-Crystal Metallic Nanowires and Metal/Semiconductor Nanowire Heterostructures. *Nature* **2004**, *430*, 61–65.

(3) Zheng, Z. K.; Huang, B. B.; Qin, X. Y.; Zhang, X. Y.; Dai, Y.; Whangbo, M. H. Facile in situ Synthesis of Visible-Light Plasmonic Photocatalysts M@TiO_2 (M = Au, Pt, Ag) and Evaluation of Their Photocatalytic Oxidation of Benzene to Phenol RID H-2077-2011 RID C-1857-2008. *J. Mater. Chem.* **2011**, *21*, 9079–9087.

(4) Awazu, K.; Fujimaki, M.; Rockstuhl, C.; Tominaga, J.; Murakami, H.; Ohki, Y.; Yoshida, N.; Watanabe, T. A Plasmonic Photocatalyst Consisting of Silver Nanoparticles Embedded in Titanium Dioxide. *J. Am. Chem. Soc.* **2008**, *130*, 1676–1680.

(5) Liu, L.; Ouyang, S.; Ye, J. Gold-Nanorod-Photosensitized Titanium Dioxide with Wide-Range Visible-Light Harvesting Based on Localized Surface Plasmon Resonance. *Angew. Chem., Int. Ed.* **2013**, *52*, 6689–6693.

(6) Linic, S.; Christopher, P.; Ingram, D. B. Plasmonic-Metal Nanostructures for Efficient Conversion of Solar to Chemical Energy. *Nat. Mater.* **2011**, *10*, 911–921.

(7) Mubeen, S.; Lee, J.; Singh, N.; Kramer, S.; Stucky, G. D.; Moskovits, M. An Autonomous Photosynthetic Device in Which All Charge Carriers Derive from Surface Plasmons. *Nat. Nanotechnol.* **2013**, *8*, 247–251.

(8) Schuck, P. J. Nanoimaging: Hot Electrons Go through the Barrier. *Nat. Nanotechnol.* **2013**, *8*, 799–800.

(9) Janotti, A.; Varley, J. B.; Rinke, P.; Umezawa, N.; Kresse, G.; Van de Walle, C. G. Hybrid Functional Studies of the Oxygen Vacancy in TiO_2. *Phys. Rev. B: Condens. Matter Mater. Phys.* **2010**, *81*, 085212–085212.

(10) Zhang, Z.; Yates, J. T. Band Bending in Semiconductors: Chemical and Physical Consequences at Surfaces and Interfaces. *Chem. Rev. (Washington, DC, U.S.)* **2012**, *112*, 5520–5551.

(11) Hodak, J. H.; Martini, I.; Hartland, G. V. Spectroscopy and Dynamics of Nanometer-Sized Noble Metal Particles. *J. Phys. Chem. B* **1998**, *102*, 6958–6967.

(12) Bian, Z.; Tachikawa, T.; Zhang, P.; Fujitsuka, M.; Majima, T. Au/TiO_2 Superstructure-Based Plasmonic Photocatalysts Exhibiting Efficient Charge Separation and Unprecedented Activity. *J. Am. Chem. Soc.* **2014**, *136*, 458–465.

(13) Kelly, K. L.; Coronado, E.; Zhao, L. L.; Schatz, G. C. The Optical Properties of Metal Nanoparticles: The Influence of Size, Shape, and Dielectric Environment. *J. Phys. Chem. B* **2002**, *107*, 668–677.

(14) Song, P.; Nordlander, P.; Gao, S. Quantum Mechanical Study of the Coupling of Plasmon Excitations to Atomic-Scale Electron Transport. *J. Chem. Phys.* **2011**, *134*, 074701.

(15) Kresse, G.; Hafner, J. Ab Initio Molecular Dynamics for Liquid Metals. *Phys. Rev. B: Condens. Matter Mater. Phys.* **1993**, *47*, 558–561.

(16) Kresse, G.; Furthmüller, J. Efficient Iterative Schemes for Ab Initio Total-Energy Calculations using A Plane-Wave Basis Set. *Phys. Rev. B: Condens. Matter Mater. Phys.* **1996**, *54*, 11169–11186.

(17) Schossberger, F. Ueber die Umwandlung des Titandioxyds. *Z. Kristallogr., Kristallgeom., Kristallphys., Kristallchem.* **1942**, *104*, 358–374.

(18) Heyd, J.; Scuseria, G. E.; Ernzerhof, M. Erratum: "Hybrid Functionals Based on A Screened Coulomb Potential". *J. Chem. Phys.* **2003**, *118*, 8207; *J. Chem. Phys.* **2006**, *124*, 219906–219906.

(19) Heyd, J.; Scuseria, G. E.; Ernzerhof, M. Hybrid Functionals Based on A Screened Coulomb Potential. *J. Chem. Phys.* **2003**, *118*, 8207–8215.

(20) Monkhorst, H. J.; Pack, J. D. Special Points for Brillouin-Zone Integrations. *Phys. Rev. B: Solid State* **1976**, *13*, 5188−5192.
(21) Blöchl, P. E.; Jepsen, O.; Andersen, O. K. Improved Tetrahedron Method for Brillouin-Zone Integrations. *Phys. Rev. B: Condens. Matter Mater. Phys.* **1994**, *49*, 16223−16233.
(22) Van de Walle, C. G.; Neugebauer, J. Universal Alignment of Hydrogen Levels in Semiconductors, Insulators, and Solutions. *Nature* **2003**, *423*, 626−628.
(23) Mattioli, G.; Alippi, P.; Filippone, F.; Caminiti, R.; Amore Bonapasta, A. Deep versus Shallow Behavior of Intrinsic Defects in Rutile and Anatase TiO_2 Polymorphs. *J. Phys. Chem. C* **2010**, *114*, 21694−21704.
(24) Purcell, E. M.; Pennypacker, C. R. Scattering and Absorption of Light by Nonspherical Dielectric Grains. *Astrophys. J.* **1973**, *186*, 705−714.
(25) Draine, B. T. The Discrete-Dipole Approximation and Its Application to Interstellar Graphite Grains. *Astrophys. J.* **1988**, *333*, 848−872.
(26) Johnson, P. B.; Christy, R. W. Optical Constants of the Noble Metals. *Phys. Rev. B: Solid State* **1972**, *6*, 4370−4379.
(27) Jellison, G. E.; Boatner, L. A.; Budai, J. D.; Jeong, B. S.; Norton, D. P. Spectroscopic Ellipsometry of Thin Film and Bulk Anatase (TiO_2). *J. Appl. Phys. (Melville, NY, U.S.)* **2003**, *93*, 9537−9541.
(28) Diebold, U. The Surface Science of Titanium Dioxide. *Surf. Sci. Rep.* **2003**, *48*, 53−229.
(29) Scheiber, P.; Fidler, M.; Dulub, O.; Schmid, M.; Diebold, U.; Hou, W.; Aschauer, U.; Selloni, A. (Sub)Surface Mobility of Oxygen Vacancies at the TiO_2 Anatase (101) Surface. *Phys. Rev. Lett.* **2012**, *109*, 136103−136103.
(30) Cheng, H.; Selloni, A. Surface and Subsurface Oxygen Vacancies in Anatase TiO_2 and Differences with Rutile. *Phys. Rev. B: Condens. Matter Mater. Phys.* **2009**, *79*, 092101−092101.
(31) Ma, X.; Dai, Y.; Guo, M.; Huang, B. Insights into the Role of Surface Distortion in Promoting the Separation and Transfer of Photogenerated Carriers in Anatase TiO_2. *J. Phys. Chem. C* **2013**, *117*, 24496−24502.
(32) Ma, X.; Dai, Y.; Guo, M.; Huang, B. Relative Photooxidation and Photoreduction Activities of the {100}, {101}, and {001} Surfaces of Anatase TiO_2. *Langmuir* **2013**, *29*, 13647−13654.
(33) Vittadini, A.; Selloni, A. Small Gold Clusters on Stoichiometric and Defected TiO_2 Anatase (101) and Their Interaction with CO: A Density Functional Study. *J. Chem. Phys.* **2002**, *117*, 353−361.
(34) Huheey, J. E. *Inorganic Chemistry*, 3rd ed; Harper & Row: New York, 1983.
(35) Wentzel, G. Eine Verallgemeinerung der Quantenbedingungen für die Zwecke der Wellenmechanik. *Z. Phys. A: Hadrons Nucl.* **1926**, *38*, 518−529.
(36) Giugni, A.; Torre, B.; Toma, A.; Francardi, M.; Malerba, M.; Alabastri, A.; ZaccariaR, P.; I, S.; FabrizioE, D. Hot-Electron Nanoscopy Using Adiabatic Compression of Surface Plasmons. *Nat. Nanotechnol.* **2013**, *8*, 845−852.
(37) Lazzeri, M.; Selloni, A. Stress-Driven Reconstruction of an Oxide Surface: The Anatase TiO_2 (001)−(1 × 4) Surface. *Phys. Rev. Lett.* **2001**, *87*, 266105−266105.
(38) Miljevic, M.; Geiseler, B.; Bergfeldt, T.; Bockstaller, P.; Fruk, L. Enhanced Photocatalytic Activity of Au/TiO_2 Nanocomposite Prepared Using Bifunctional Bridging Linker. *Adv. Funct. Mater.* **2014**, *24*, 907−915.
(39) Ma, X.; Dai, Y.; Yu, L.; Lou, Z.; Huang, B.; Whangbo, M. On the Electron−Hole Pair Generation of the Visible-Light Plasmonic Photocatalyst Ag@AgCl: Enhanced Optical Transitions Involving Mid-Gap Defect States of AgCl. *J. Phys. Chem. C* **2014**, *118*, 12133−12140.
(40) Wang, Y.; Yu, J.; Xiao, W.; Li, Q. Microwave-Assisted Hydrothermal Synthesis of Graphene Based Au−TiO_2 Photocatalysts for Efficient Visible-Light Hydrogen Production. *J. Mater. Chem. A* **2014**, *2*, 3847−3855.
(41) Liu, Z.; Hou, W.; Pavaskar, P.; Aykol, M.; Cronin, S. B. Plasmon Resonant Enhancement of Photocatalytic Water Splitting Under Visible Illumination. *Nano Lett.* **2011**, *11*, 1111−1116.
(42) Kowalska, E.; Abe, R.; Ohtani, B. Visible Light-Induced Photocatalytic Reaction of Gold-Modified Titanium(IV) Oxide Particles: Action Spectrum Analysis. *Chem. Commun. (Cambridge, U.K.)* **2009**, 241−243.